JBC RESEARCH ARTICLE

# The deubiquitinase USP28 maintains the expression of the transcription factor MYCN and is essential in neuroblastoma cells

Received for publication, December 27, 2022, and in revised form, May 10, 2023 Published, Papers in Press, May 23, 2023,
https://doi.org/10.1016/j.jbc.2023.104856

**Junjun Li[1,2,‡], Jin Peng[1,‡], Lingzhi Wu[1], Xiang Shen[3], Xinghua Zhen[1], Yimao Zhang[4], Huailu Ma[5], Yongfeng Xu[2], Qunli Xiong[2], Qing Zhu[2,*], and Pumin Zhang[1,5,6,*]**

*From the [1]Zhejiang Provincial Key Laboratory of Pancreatic Disease, The First Affiliated Hospital of Zhejiang University School of Medicine, Hangzhou, Zhejiang, China; [2]Department of Abdominal Oncology, West China Hospital, Sichuan University, Chengdu, China; [3]Chaser Therapeutics Inc., Hangzhou, Zhejiang, China; [4]Department of Pediatric Surgery, West China Hospital, Sichuan University, Chengdu, China; [5]Institute of Translational Medicine, Zhejiang University Medical School, Hangzhou, Zhejiang, China; [6]Cancer Center, Zhejiang University, Hangzhou, Zhejiang, China*

Reviewed by members of the JBC Editorial Board. Edited by George DeMartino

**Neuroblastoma (NB) is one of the most common extracranial solid tumors in children. *MYCN* gene amplification is highly associated with poor prognosis in high-risk NB patients. In non-MYCN-amplified high-risk NB patients, the expression of *c-MYC* (*MYCC*) and its target genes is highly elevated. USP28 as a deubiquitinase is known to regulate the stability of MYCC. We show here USP28 also regulates the stability of MYCN. Genetic depletion or pharmacologic inhibition of the deubiquitinase strongly destabilizes MYCN and stops the growth of NB cells that overexpress *MYCN*. In addition, *MYCC* could be similarly destabilized in non-MYCN NB cells by compromising *USP28* function. Our results strongly suggest USP28 as a therapeutic target for NB with or without MYCN amplification/overexpression.**

Neuroblastoma (NB) is one of the most common extracranial solid tumors in children, arising from the embryonic neural crest (1, 2). It accounts for approximately 7% to 8% of pediatric malignancies and about 15% of malignant neoplasm deaths in childhood (3, 4). The disease is difficult to treat and is often accompanied with poor prognosis. Currently, a combination of chemotherapy, surgery, and radiotherapy is the main treatment strategy. Key genetic aberrations in NB pathogenesis and progression include *MYCN* amplification, *TERT* rearrangements, *ALK* mutation/amplification, mutations in *TP53*, *KRAS, NRAS, ATRX*, etc. (5–8). The amplification of *MYCN* is observed in 20% to 30% of cases and confers poor prognosis (9, 10). In addition, about 11% of high-risk NB cases show augmented expression of *c-Myc* (*MYCC*) (11). *MYCN* and *MYCC* belong to the Myc family of transcription factors that are critical in promoting cell growth and proliferation (12–14). Thus, it is apparent that targeting *MYCN* (or *MYCC*) would bring therapeutic benefits for NB patient (15). However, direct targeting of MYC proteins has been proven difficult, if not impossible (16–18).

*USP28* (ubiquitin specific protease 28) is a deubiquitinase which is increasingly found involved in tumorigenesis (19). It is not an oncogene by itself, but it can help a number of oncogenic proteins stay away from ubiquitination and subsequent proteasomal degradation (20). c-MYC, NOTCH1, LSD1, c-JUN, HIF1A, and TCF/LEF family transcription factors are some of those proteins reported (20–24). Many of these proteins are ubiquitinated by the E3 ubiquitin ligase $SCF^{FBW7}$ (25). Thus, FBW7-USP28 seems to work together to maintain the homeostasis of these proteins (26). We reported previously that targeting USP28 with a potent small molecule inhibitor we developed, could dramatically downregulate c-MYC in tumor cell lines originated across many different tissue types and bring the growth of these cells to a halt (27), indicating that inhibiting USP28 is a valid approach to interfere with c-MYC function. Given the similarity between *MYCC* and *MYCN*, it is not surprising that MYCN was found to also undergo FBW7-mediated ubiquitination and degradation (28). Therefore, it is reasonable to assume that targeting USP28 would downregulate MYCN as well.

Here we report that *USP28* is critical for the survival of NB cells. Genetic depletion or pharmacologic inhibition of the deubiquitinase enhances MYCN ubiquitination and degradation, resulting in apoptotic cell death in *MYCN*-amplified NB cells. Further, for those NB cells without *MYCN* amplification, targeting *USP28* is still effective as c-MYC now becomes unstable. Together, our results suggest targeting USP28 as a potential treatment for NB.

## Results

### *USP28 maintains MYCN expression in NB cells*

To determine the function of *USP28* in regulating *MYCN*, we first looked for NB cell lines that overexpressed *MYCN*. As

‡ These authors contributed equally to this work.
* For correspondence: Pumin Zhang, pzhangbcm@zju.edu.cn; Qing Zhu, newzhuqing1972@163.com.
Present address for Junjun Li: Department of Radiation Oncology, Shanghai General Hospital, Shanghai Jiao Tong University School of Medicine, Shanghai 200080, China.

shown in Figure 1*A*, both IMR32 and SK-N-BE (2) highly express *MYCN* but not *MYCC,* whereas SK-N-SH, SK-N-AS, and SH-SY-5Y are opposite to IMR32 and SK-N-BE (2) with little expression of *MYCN* but high levels of *MYCC* expression. As expected, depleting the expression of *USP28* (with two shRNAs targeting different regions of the DUB) resulted in the downregulation of MYCN (Fig. 1*B*), and the downregulation could be rescued by the addition of proteasome inhibitor MG132 in the culture medium (Fig. 1*C*).

The data above indicate that MYCN is degraded through ubiquitin-proteasome system and suggest that USP28 is a deubiquitinase for MYCN. Indeed, as shown in Fig. 1*D*, when the expression of *USP28* is depleted with the same two shRNAs (Fig. 1*B*) in HEK293 cells, MYCN ubiquitination increased significantly. On the other hand, the overexpression of *USP28*, but not that of the catalytically inactive form of USP28 (USP28-C171A), was able to suppress the ubiquitination (Fig. 1*E*). Furthermore, we expressed Flag-MYCN and HA-ubiquitin in HEK293 cells, immunoprecipitated MYCN with anti-Flag beads, and incubated the immunoprecipitates with control, purified USP28, or purified USP28 premixed with its inhibitor CT1113 (27). After the incubation, the immunoprecipitates were run in a gel and the amount of ubiquitination on MYCN was quantitated through Western blotting. As expected, the purified USP28 could remove the ubiquitination on MYCN but such a removal was greatly suppressed by CT1113 (Fig. 1*F*). Taken together, these data demonstrate that USP28 is a deubiquitinase that regulates the expression of MYCN.

As a deubiquitinase for MYCN, USP28 should be able to interact with it. To demonstrate that, we resorted to reciprocal immunoprecipitation. As shown in Figure 2*A*, USP28 could bring down MYCN and vice versa in HEK293 cells expressing Flag-MYCN. An interaction between endogenous MYCN and USP28 could also be detected in IMR32 cells (Fig. 2*B*). We further mapped the region in USP28 that could mediate the interaction (Fig. 2*C*). Different regions of USP28 were Flag-tagged and expressed together with MYCN-GFP in HEK293 cells and immunoprecipitated with anti-Flag antibodies. It is apparent that the USP domain of USP28 interacts with MYCN.

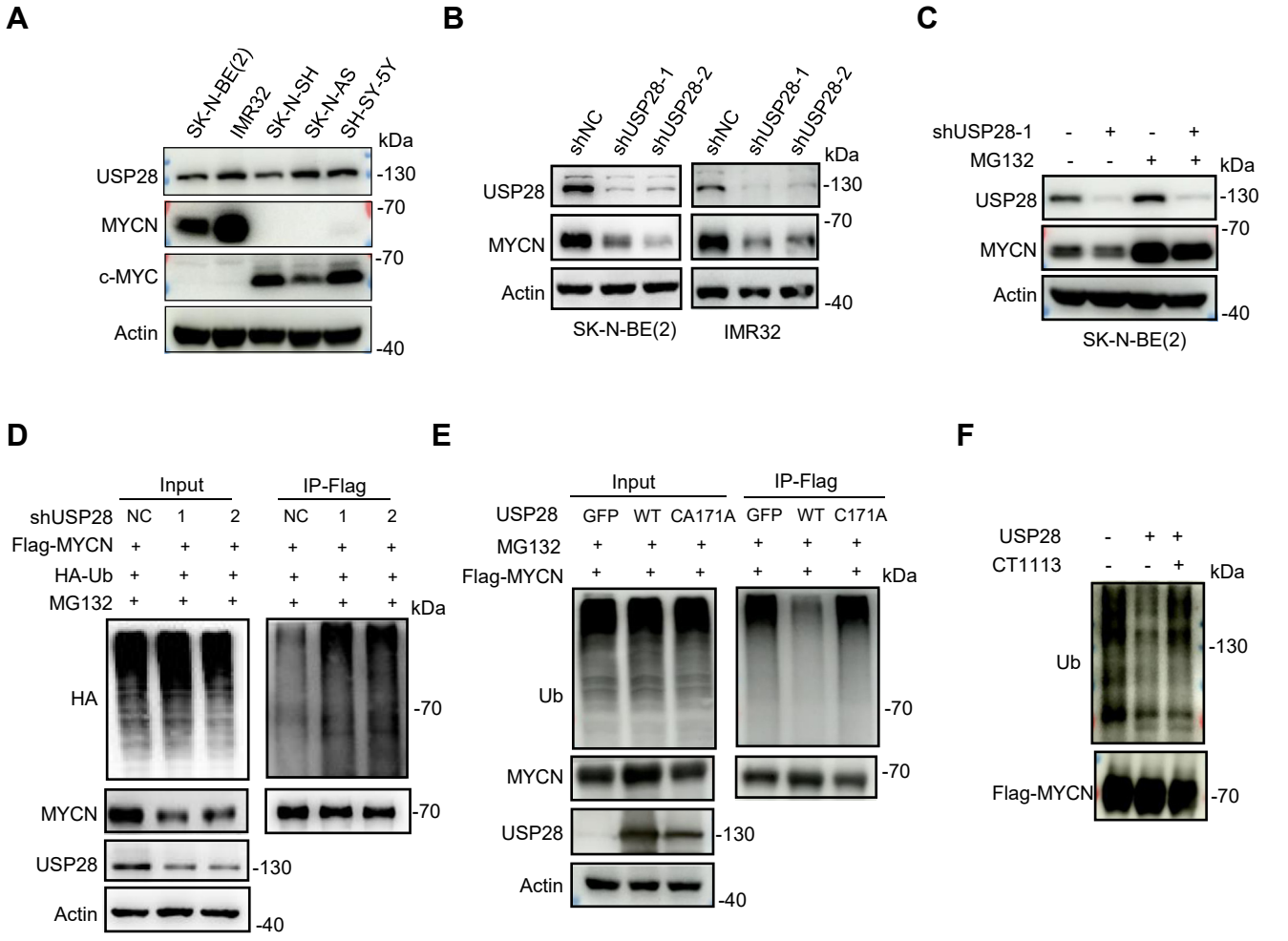


**Figure 1. USP28 maintains MYCN expression.** *A*, immunoblotting analysis of the expression of USP28, MYCN and c-MYC in SK-N-BE (2), IMR32, SK-N-SH, SK-N-AS, and SK-SY-5Y cells. *B*, immunoblotting analysis of MYCN in the SK-N-BE (2) and IMR32 cells depleted of *USP28* expression *via* two independent shRNAs. *C*, treatment with proteasome inhibitor MG132 in SK-N-BE (2) cells prevented the degradation of MYCN. *D*, the ubiquitination assay of MYCN in *USP28*-depleted 293T cells. *E*, the ubiquitination assay of MYCN in *USP28* (WT or C171A mutant)–overexpressing 293T cells. *F*, *in vitro* deubiquitination by USP28. Flag-MYCN and HA-ubiquitin were expressed in 293T cells. Flag-MYCN (including ubiquitinated form) was pulled down and incubated with 1 μM purified USP28 with or without premixing with 50 μM CT1113. USP28, ubiquitin specific protease 28.

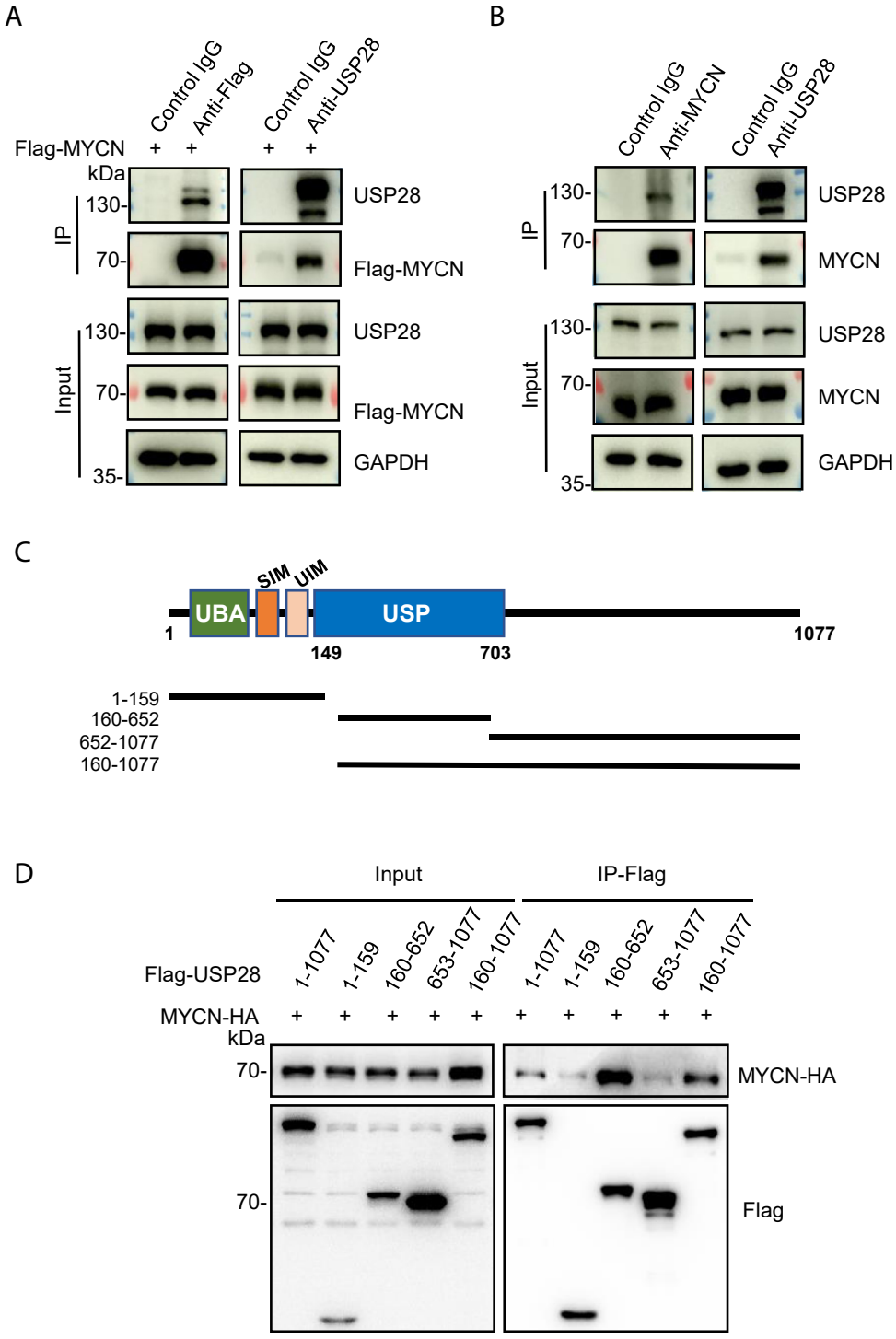


**Figure 2. USP28 maintains MYCN expression in neuroblastoma cells.** *A*, USP28 interacts with MYCN. Flag-MYCN expressed in 293T cells or endogenous USP28 was immunoprecipitated, and the immunoprecipitates were analyzed. *B*, the interaction between endogenous MYCN and USP28 in IMR32 cells were analyzed through IP-Western blotting. *C*, schematic diagrams showing USP28 fragments. *D*, detection of the interaction of USP28 fragments in (*C*) with MYCN in 293T cells. USP28, ubiquitin specific protease 28.

### *USP28 is essential for the survival of NB cells with MYCN overexpression*

Given the critical role of *MYCN* in NB cells (29, 30), we wondered what would happen to the *USP28*-depleted cells now with destabilized MYCN. Not surprisingly, both SK-N-BE (2) and IMR32 could barely grow when *USP28* was knocked down with the same shRNAs as above (Fig. 3*A*). The cells died over time through apoptosis (Fig. 3*B*). The apoptosis marker, cleaved PARP, increased significantly in *USP28*-depleted cells (Fig. 3*C*). We could also see a dramatic decrease of cyclin D1 expression as expected of downregulation of *MYCN* (Fig. 3*C*).

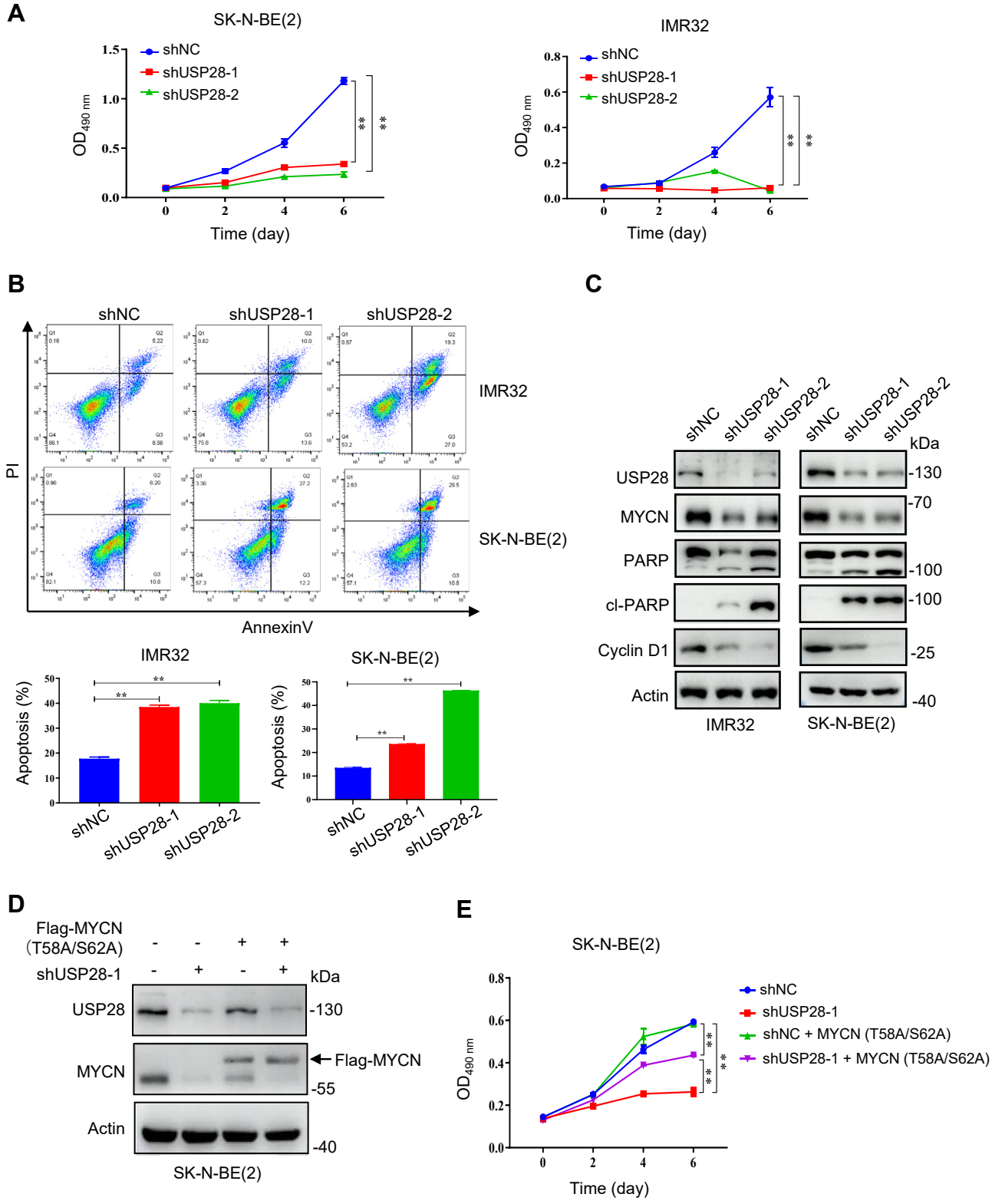


**Figure 3. USP28 is essential for the survival of neuroblastoma cells with MYCN overexpression.** *A*, cell viability assay of SK-N-BE (2) and IMR32 cells depleted of *USP28* expression. The experiment was performed at least three times. A typical result was shown. Error bars denote S.D. *B*, flow cytometry analysis of apoptosis in SK-N-BE (2) and IMR32 cells depleted of *USP28* expression. Apoptotic population was the sum of the two quadrats on the *right* in each FACS diagram. Error bars denote S.E.M. *C*, Western blotting analysis of the expression of the indicated proteins in SK-N-BE (2) and IMR32 cells depleted of *USP28* expression. *D*, Western blotting analysis documenting the expression of exogenous $MYCN^{T58A/S62A}$. *E*, growth curve analysis of SK-N-BE (2) cells with *USP28* depletion and the expression of $MYCN^{T58A/S62A}$. Student's *t* tests were performed to obtain statistical significance. **indicates $p < 0.01$; ns: $p \geq 0.05$. USP28, ubiquitin specific protease 28.

Furthermore, the growth suppression effect of *USP28* depletion could be largely rescued by exogenous expression of a mutant form of *MYCN* in which two residues (T58 and S62) were mutated to Ala (Fig. 3, *D* and *E*). It is known that phosphorylation of T58 and S62 is required for MYCN ubiquitination by FBW7 (31). Thus, $MYCN^{T58A/S62A}$ is resistant to ubiquitin-mediated proteasomal degradation, and no longer requires *USP28* for stabilization. However, $MYCN^{T58A/S62A}$ expression did not fully rescue the growth deficiency caused by *USP28* depletion, probably because the exogenous expression could not reach to the level of endogenous *MYCN* (Fig. 3*D*).

### Pharmacologic inhibition of USP28 blocks the growth of NB with MYCN overexpression

The results above strongly suggest that USP28 is a target against NB. To test that, we took advantage of the potent USP28 inhibitor CT1113 we had developed (27). Indeed, treating SK-N-BE (2) and IMR32 cells with CT1113 downregulated MYCN protein levels in a dose-dependent manner (Fig. 4*A*). Another known substrate of USP28, LSD1, was downregulated as well (Fig. 4*A*). USP28 itself also decreased since it is its own deubiquitinase. Accordingly, these two NB cell lines are very sensitive to CT1113 treatment (Fig. 4*B*). They could not grow at all in the presence of 200 nM or more CT1113 and grew poorly with 100 nM. As with *USP28* depletion, the cells died by apoptosis (Fig. 4*C*). Indeed, CT1113 treatment increased the levels of cleaved PARP as expected (Fig. 4*D*). Further, the expression of $MYCN^{T58A/S62A}$ in IMR32 cells made the cells more resistant to CT1113, suggesting that CT1113 works through MYCN, at least partially (Fig. 4*E*).

Next, we tested the efficacy of CT1113 *in vivo*. SK-N-BE (2) cells were inoculated in nude mice subcutaneously to from a tumor first. The tumor was then harvested, divided into small pieces, and reinoculated. When the inoculated pieces grew to palpable sizes (~100 $mm^3$), the nude mice were randomly grouped and treated with vehicle or CT1113 at 15 or 20 mg/kg body weight twice a day. After 10 to 14 days, the mice were sacrificed, and the tumors were harvested for analyses. As shown in Figure 5*A*, CT1113 was very effective in blocking the tumor growth, and the effect was dose-dependent. CT1113 significantly suppressed tumor proliferation as indicated by Ki67 staining (Fig. 5*B*). As expected, MYCN levels in the tumor were greatly downregulated by CT1113 treatment (Fig. 5*C*). Further, CT1113 was tested against a patient-derived xenograft (PDX) model of NB. Again, the USP28 inhibitor was extremely efficacious (Fig. 5*D*). This PDX model apparently was derived from a MYCN-type tumor as MYCN was readily detectable while c-MYC was absent in the tumor samples collected from the mice (Fig. 5*E*). Again, CT1113 treatment effectively lowered the expression levels of MYCN in the tumors (Fig. 5*E*).

### USP28 is also critical for the non-MYCN NB cells

Not all NB were driven by *MYCN* amplification or overexpression. In those non-*MYCN* NB cells (Fig. 1*A*), we wonder whether targeting *USP28* would be as effective as in *MYCN* cells, since USP28 might be required to maintain their *MYCC* expression as in many other types of tumor cells we have tested (27). To that end, we first employed RNA interference to deplete *USP28* expression. Indeed, knocking down *USP28* caused c-MYC levels to decrease dramatically, so did LSD1 levels in both SK-N-SH and SK-N-AS cells (Fig. 6*A*). These cells failed to grow (Fig. 6*B*) and died by apoptosis overtime (Fig. 6, *C* and *D*). Further, CT1113 treatment was able to suppress MYCC expression as well as that of LSD1 as expected (Fig. 6*E*), blocking the growth (Fig. 6*F*), and causing cell death (Fig. 6, *G* and *H*).

We further tested CT1113 against the tumors formed by SK-N-SH and SK-N-AS cells. As shown Fig. 7*A*, the compound was very effective in suppressing the tumor growth derived from SK-N-AS cells. MYCC and LSD1 were suppressed in the tumors as expected (Fig. 7*B*). CT1113 was also efficacious against the tumors formed by SK-N-SH cells (Fig. 7*C*).

## Discussion

NB is a devastating disease in children (32, 33). It is driven by different oncogenic pathways and displays high heterogeneity in its pathogenesis that limits treatment options (34). In fact, chemotherapy is still the most often prescribed for the patients. Thus, targeted therapies are in urgent need. However, finding suitable targets for NB is hindered by the fact that a diverse set of genetic alterations are found responsible for the disease. Since MYC (MYCC or MYCN) is ultimately required for NB cells to grow and proliferate, just like the cells from any other types of malignancies, targeting MYC would be of high therapeutic value. We show here that genetic depletion or pharmacologic inhibition of *USP28* can destabilize MYCN and lower its expression to such a level that is no longer sufficient to sustain cell growth and proliferation.

Tavana *et al.* (35) reported previously that USP7 could act as a deubiquitinase for MYCN. It is possible that both USP7 and USP28 contribute to the regulation of MYCN ubiquitination. However, targeting USP28 brings additional therapeutic benefits since USP28 also regulates MYCC stability and thus could be useful against non-MYCN NB (Figs. 6 and 7). Moreover, in addition to MYC, LSD1 was also downregulated when USP28 was targeted (Fig. 6*A*). It is known that LSD1 is highly expressed in poorly differentiated NB and interfering its function impairs the growth of NB cells (36). Thus, we believe USP28 is a better target for NB.

The past 2 decades have witnessed the rise and success of targeted therapies designed to block key oncodrivers like EGFR, HER2, etc. However, most (if not all) such druggable targets have been discovered and tried already, and yet, there are still tremendous unmet needs in the clinic such as NB that call for new therapeutic targets. In addition to the driver oncogenes, cancer cells also addict to certain nononcogenes which are required to maintain their transformed phenotypes and to deal with the cellular stresses that come with the transformation process (37). In theory, targeting those addicted nononcogene products should be as effective as targeting

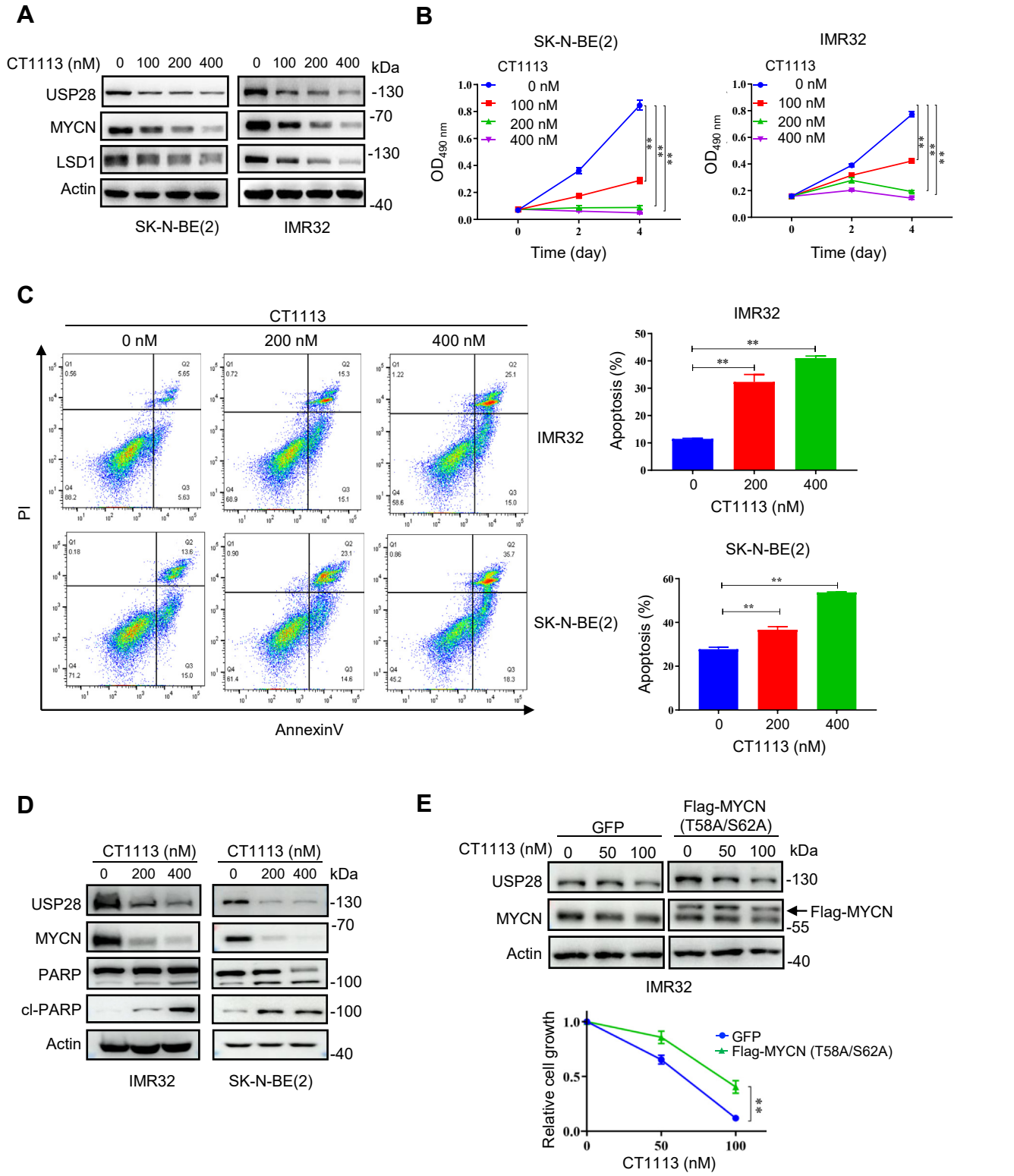


**Figure 4. Pharmacologic inhibition of USP28 blocks the growth of neuroblastoma cells with MYCN overexpression.** *A*, Western blotting analysis of the expression of the indicated proteins in SK-N-BE (2) and IMR32 cells treated with CT1113 for 96 h. *B*, cell viability assay of SK-N-BE (2) and IMR32 cells treated with CT1113 for different periods of time. *C*, flow cytometry analysis of apoptosis in SK-N-BE (2) and IMR32 cells treated with CT1113 for 96 h. The percentage of apoptotic cells were quantified and plotted. Apoptotic population was the sum of the two quadrats on the right in each FACS diagram. Error bars indicate S.E.M. *D*, Western blotting analysis documenting the expression of the apoptosis marker, cleaved PARP (cl-PARP), in SK-N-BE (2) and IMR32 cells treated with CT1113 for 96 h. *E*, CT1113 treatment of IMR32 cells expressing Flag-MYCN (T58A/S62A) or GFP. The expression of Flag-MYCN (T58A/S62A) was analyzed with immunoblotting and the cell growth monitored *via* the cell viability assay. Student's *t* tests were performed to obtain statistical significance. **indicates $p < 0.01$; ns: $p \geq 0.05$. USP28, ubiquitin specific protease 28.

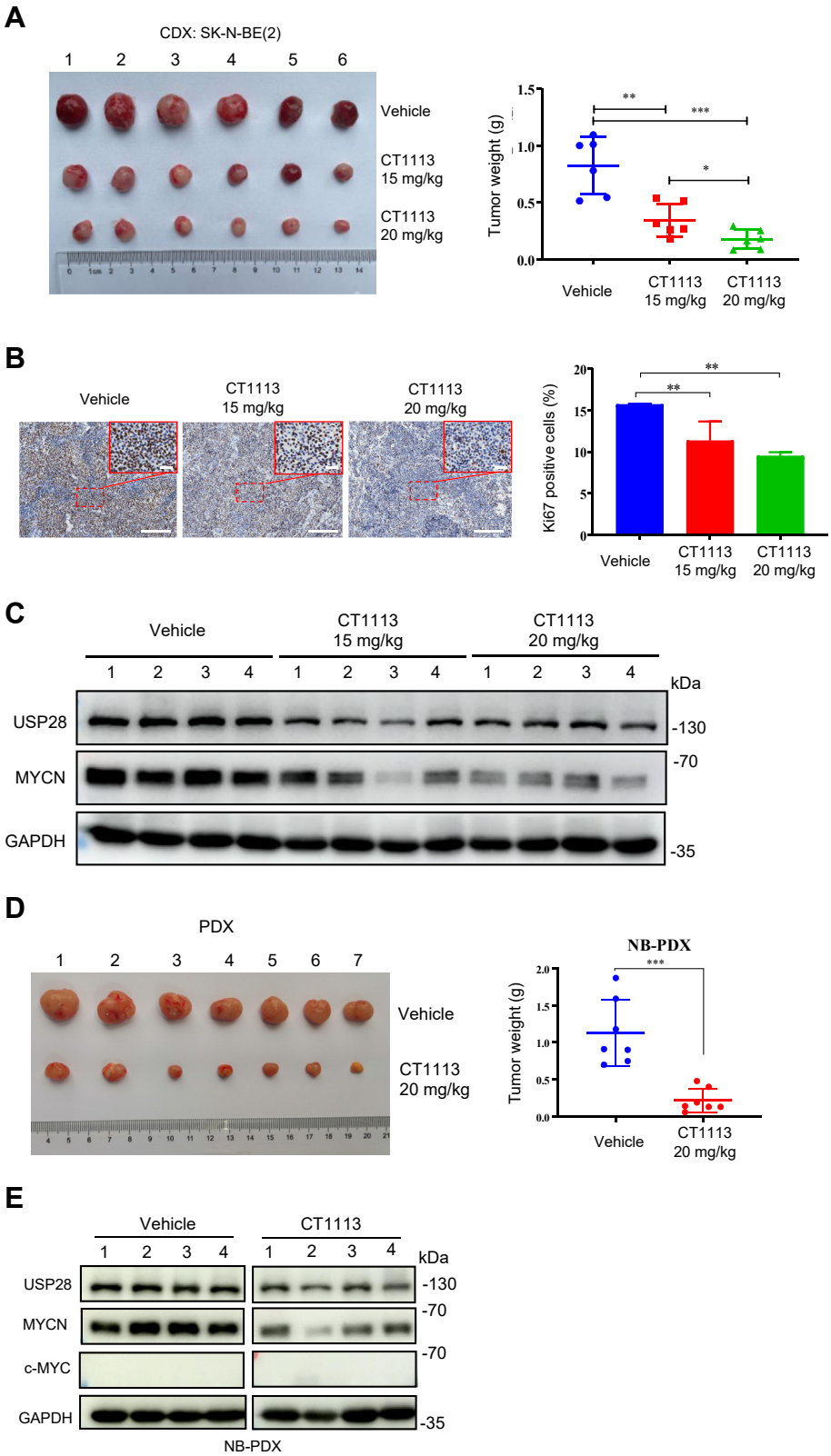


**Figure 5. Neuroblastoma xenografts are responsive to USP28 inhibitor treatment.** *A*, images of SK-N-BE (2) xenograft tumors after a 12 days treatment with CT1113 or vehicle control. The tumor weight was plotted. Error bars denote S.D. *B*, representative microimages of immunohistochemical staining of Ki-67. Ki-67-positive cells were counted, and the percentages were plotted (10X, scale bar 200 μm; 50X, scale bar 40 μm). Error bars indicate S.E.M. *C*, Western blotting analysis of the expression of USP28 and MYCN in SK-N-BE (2) tumors in (*A*). *D*, images of PDX tumors after a 21 days treatment with CT1113 or vehicle control. The tumor weight was plotted. Error bars denote S.D. *E*, Western blotting analysis of the expression of USP28, MYCN, and c-MYC in PDX tumors from (*D*). Student's *t* tests were performed to obtain statistical significance. *** indicates $p < 0.001$; **$p < 0.01$; *$p < 0.05$; ns: $p \geq 0.05$. USP28, ubiquitin specific protease 28.

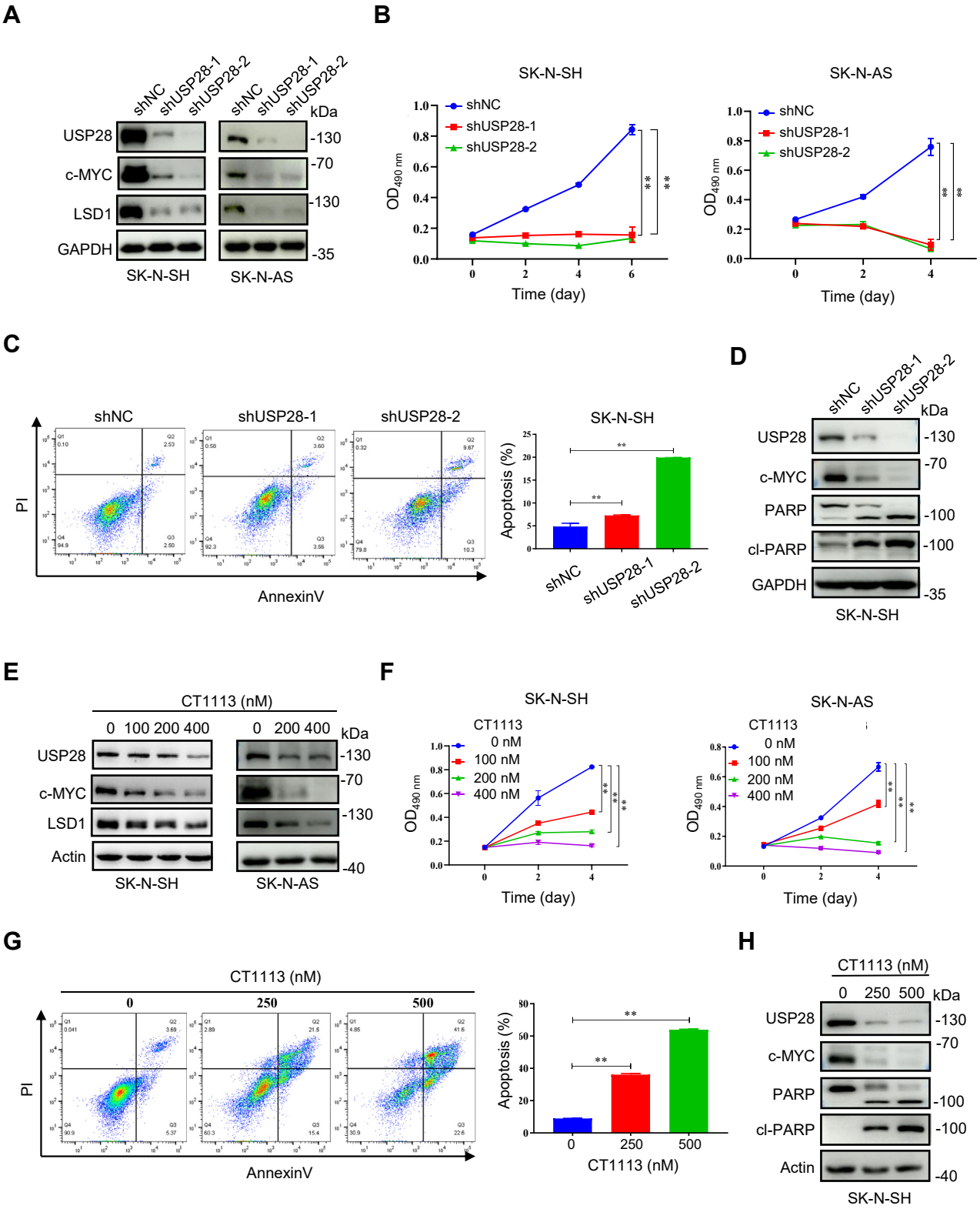


**Figure 6. USP28 is also critical for the non-MYCN neuroblastoma cells *in vitro*.** *A*, Western blotting analysis of c-MYC and LSD1 in SK-N-SH and SK-N-AS cells depleted of *USP28*. *B*, cell viability assay of SK-N-SH and SK-N-AS cells depleted of *USP28*. *C*, flow cytometry analysis of apoptosis in SK-N-SH cells depleted of *USP28*. Apoptotic population was the sum of the two quadrats on the *right* in each FACS diagram. Error bars denote S.E.M. *D*, Western blotting analysis documenting the expression of the apoptosis marker, cleaved PARP (cl-PARP), in SK-N-SH cells depleted of *USP28*. *E*, Western blotting analysis of the expression of the indicated proteins in SK-N-SH and SK-N-AS cells treated with CT1113 for 96 h. *F*, cell viability assay of SK-N-SH and SK-N-AS cells treated with CT1113 for different periods of time. *G*, flow cytometry analysis of apoptosis in SK-N-SH cells treated with CT1113 for 96 h. The percentage of apoptotic cells were quantified and plotted. Apoptotic population was the sum of the two quadrats on the right in each FACS diagram. Error bars indicate S.E.M. *H*, Western blotting analysis documenting the expression of the apoptosis marker, cleaved PARP (cl-PARP), in SK-N-SH cells treated with CT1113 for 96 h. Student's *t* tests were performed to obtain statistical significance. ** indicates $p < 0.01$; ns: $p \geq 0.05$. USP28, ubiquitin specific protease 28.

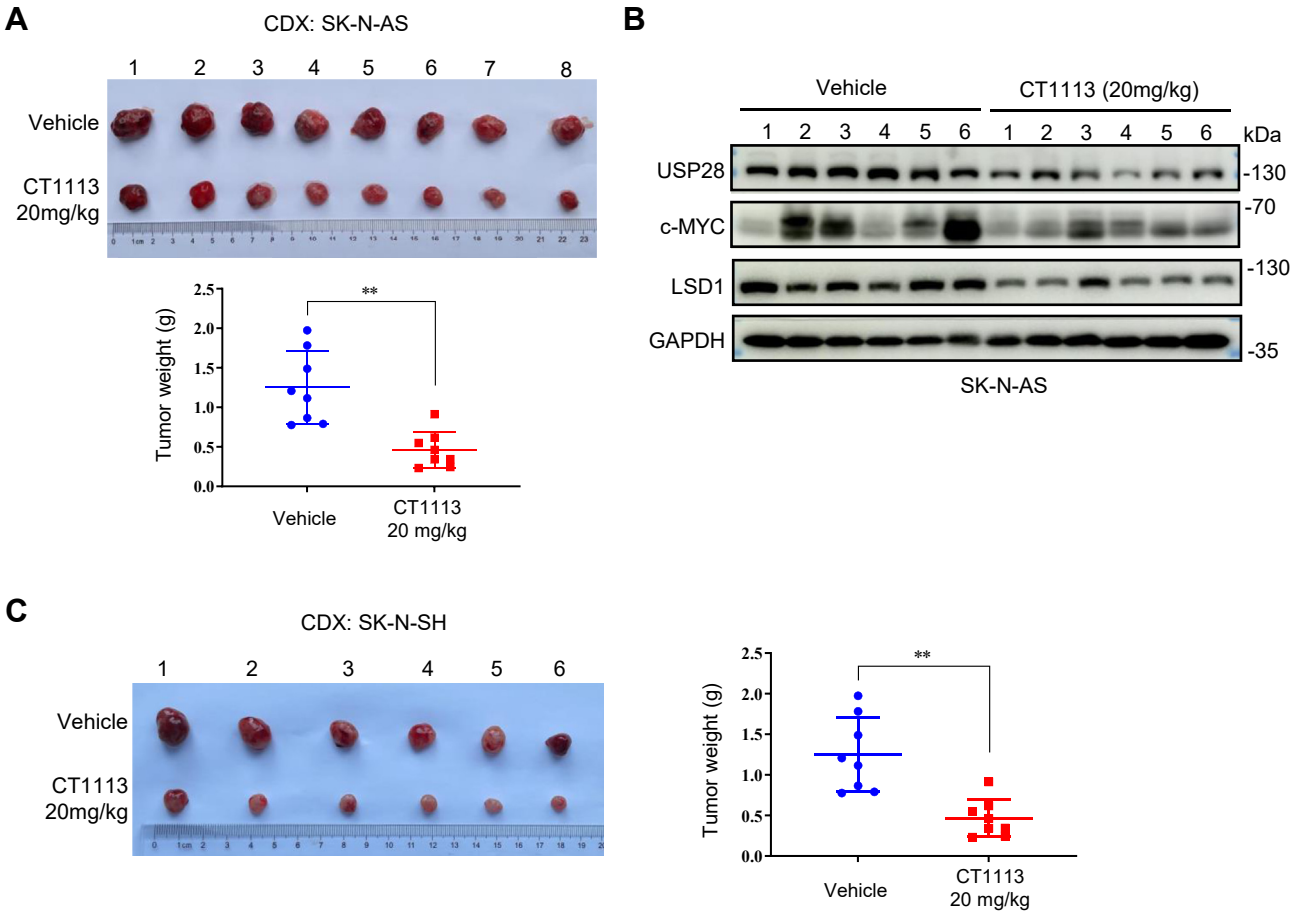


**Figure 7. Non-MYCN neuroblastoma xenografts are responsive to USP28 inhibitor treatment.** *A*, images of SK-N-AS xenograft tumors after a 12 days treatment with CT1113 or vehicle control. The tumor weight was plotted. Error bars denote S.D. *B*, Western blotting analysis of the expression of USP28, c-MYC, and LSD1 in SK-N-AS tumors in (*A*). *C*, images of SK-N-SH xenograft tumors after a 12 days-treatment with CT1113 or vehicle control. The tumor weight was plotted. Error bars denote S.D. Student's *t* tests were performed to obtain statistical significance. ** indicates $p < 0.01$; ns: $p \geq 0.05$. USP28, ubiquitin specific protease 28.

driver oncoproteins, and such a strategy might prove to be particularly beneficial in situations where therapeutic targets are hard to come by. USP28 seems to be such a nononcogene target in NB and in other malignancies (24, 27, 38–40).

## Experimental procedures

### *Cell culture*

NB cell lines, SK-N-BE (2), IMR32, SK-N-SH, SK-N-AS, and SK-SY-5Y, were purchased from the Shanghai Cell Bank, Chinese Academy of Sciences. 293T cells was obtained from the Cell Bank of Type Culture Collection of Chinese Academy of Sciences. The cells were cultured in either MEM, MEM/F12 (50:50), or Dulbecco's modified Eagle's medium supplemented with 10% fetal bovine serum, 1 μg/ml penicillin, and streptomycin. The medium, fetal bovine serum, trypsin, and penicillin-streptomycin were purchased from Gibco. All cells were maintained in an incubator supplemented with 5% $CO_2$ at 37 °C.

### *Animal experiments*

All animal experiments were approved by the Animal Care and Use Committee of the First Affiliated Hospital of Zhejiang University. The mice are purchased from Beijing Vital River Laboratory Animal Technology Co, Ltd. To generate cell-derived xenograft tumors, SK-N-BE (2), IMR32, SK-N-SH, or SK-N-AS cells ($2 \times 10^6$) were mixed at a 1:1 ratio (volume) with matrigel (BD Biosciences) and injected subcutaneously into 5∼6-weeks-old BALB/c nude mice. For the PDX model, the tumor sample from a patient with NB was placed in cold PBS, and the necrotic and fat tissues were dissected out. The remaining tumor tissue was cut into very small pieces (1–2 $mm^3$) to be engrafted subcutaneously into 5∼6-weeks-old BALB/c nude mice. When the PDX tumors grew up to ∼500 $mm^3$, they were harvested, cut into small pieces, and inoculated back to BALB/c nude mice. This process was repeated several more times to establish a PDX line. To evaluate the antitumor effect of CT1113, the inoculated tumors (cell-derived xenograft or PDX) were allowed to grow for 2 to 3 weeks to reach a size about 100 $mm^3$, and the tumor-bearing mice were then randomized into two groups. The animals were given CT1113 (20 mg/kg body weight, bid) or the vehicle by oral gavage. The growth of the tumors was monitored every 3 days with a vernier caliper. 2 to 3 weeks after the treatment, the mice were sacrificed, and the tumors were excised out and weighed.

Tumor tissues were collected and fixed in PBS-buffered 4% paraformaldehyde overnight, dehydrated, and embedded in

paraffin. Serial 5 μm sections were cut and stained with hematoxylin and eosin or processed for immunohistochemical staining of Ki67. Three view fields under a 40× objective of each section were examined and counted to obtain the percentage of Ki67-positive cells.

### Plasmids and lentiviruses

Plasmids used in this study were generated using standard cloning methods. shRNAs were constructed in pLKO.1 with the following sequences: shNC (5′-TTCTCCGAACGTGTCACGT-3′), shUSP28-1 (5′-GCACAGAAGTTCGTTGTCATA-3′), shUSP28-2 (5′-GACTGAAGATCATCCATTAAT-3′), shMYCN-1 (5′-AGCAGCAGTTGCTAAAGAAAC-3′), shMYCN-2 (5′-TGAGCGATTCAGATGATGAAC-3′), shMYCC-1 (5′-CTGAGACAGATCAGCAACAAC-3), and shMYCC-2 (5′-AGATGAGGAAGAAATCGATGC-3). The human *MYCN* cDNA was mutated with standard site-specific mutagenesis and cloned into the vector pHAGE with a Flag tag. The lentiviruses for expression of shRNAs or *MYCN* were packaged in 293T cells with standard packaging plasmids and method. Lentiviral infection of the cells was performed with standard method, and the infected cells were selected with 4 μg/ml puromycin (InvivoGen) for 2 days to obtain stable gene-knocking down or overexpression cell lines.

### Cell proliferation and apoptosis assays

For the MTS cell proliferation assay, the cells were seeded in a 96-well plate at a density of 3000 cells per well and cultured for the indicated time periods. At the end of the incubation period, the number of viable cells was determined using a colorimetric assay (MTS, Promega). In brief, the culture medium was removed, and 100 μl fresh complete culture medium plus 20 μl of MTS was added to each well. The cells were then incubated for 2 h before the absorbance of the formazan product was measured at 490 nm.

For apoptosis assay, the apoptotic cells were stained with Annexin V-FITC/PI Apoptosis Kit (MultiSciences) according to the manufacturer's instruction. The cells were analyzed on a BD FACSCanto II flow cytometer, and the data were analyzed with FlowJo software (BD Biosciences).

### Western blotting analysis and immunoprecipitation

For Western blotting analysis of proteins, the cells or tissues were lysed in RIPA buffer (Applygen Technologies Inc) supplemented with a protease inhibitor cocktail (Roche Diagnostics), and the lysates were centrifuged at high speed to remove insoluble debris. The protein concentration of the resultant lysates was determined with a bicinchoninic acid assay kit (Beyotime). Equal amounts of proteins were boiled for 5 min in 5× SDS loading buffer (Biosharp), separated in an SDS-polyacrylamide gel, and transferred onto nitrocellulose membranes. The membranes were incubated for 1 h in blocking buffer (5% nonfat dry milk in TBST) and then with primary antibodies at 4 °C overnight. After three washes with TBST, the membrane was incubated for 1 h at room temperature with horseradish peroxidase–conjugated secondary antibodies. The membrane was then washed three times and visualized with SuperSignal West Pico Chemiluminescent Substrate (Thermo Fisher Scientific). The expression of GAPDH, β-actin, or tubulin was routinely used as a loading control.

For immunoprecipitation, the cells were lysed in NETN buffer and centrifuged to remove debris. The supernatants were cell lysates. The desired protein was precipitated with appropriate antibodies conjugated directly to Sepharose beads (such as Flag M2 beads, Sigma) or *via* protein A/G-conjugated Sepharose beads. About 2 mg total protein worth of cell lysates were incubated with the antibody-conjugated beads for 1 h at room temperature or overnight at 4 °C. After the incubation, the beads were washed with NETN buffer at least three times. The beads-bound proteins were eluded off through boiling in denaturing SDS-gel loading buffer and analyzed with Western blotting.

### Ubiquitination assay

Ubiquitination assay was performed as previously described (41). HEK293T cells were transfected with Flag-MYCN and other indicated plasmids. Forty-eight hours after the transfection, the cells were treated with 10 μM MG132 for 6 to 8 h and lysed in NETN buffer (pH8.0 tris-HCl, 100 mM NaCl, 1 mM EDTA, 0.5% Nonidet P-40) containing 1% SDS and 1% sodium deoxycholate, vortexed vigorously for 15∼30 min, and boiled for 10 min. After that, 5 to 9 times of the volume of more NETN buffer were added to reduce SDS content to 0.1% and the so produced cell lysates were incubated with appropriate antibody-conjugated beads followed by the rest of immunoprecipitation procedures.

For *in vitro* deubiquitination assay, HEK293T cells grown on a 15-cm dish were transfected with 20ug Flag-MYCN plus 4ug HA-ubiquitin. Forty-eight hours after the transfection, MG132 was added to the medium to a final concentration of 10 μM, and the cells were harvested 4 h later. The cells were trypsinized, collected, washed in PBS, lysed in NETN for 30 min, and proceeded to anti-Flag immunoprecipitation procedures. The resultant Flag-MYCN beads were divided to three equal parts to be incubated with (a) 19 μl DUB assay buffer (de-ubiquitination assay buffer: 50 mM Tris HCl pH 7.5/1 mM EDTA/100 mM NaCl/0.05% CHAPS/5 mM DTT) + 1 μl DMSO; (b) 9 μl DUB assay buffer + 1 μl DMSO + 10 μl purified USP28 (His6-USP28, Cat. # E570, R&D Systems; final concentration, 1 μM); or (c) 9 μl DUB assay buffer + 10 μl USP28 (final concentration, 1 μM) + 1 μl CT1113 (final concentration, 50 μM). USP28 plus DMSO or CT1113 were preincubated at room temperature for 30 min before being added to Flag-MYCN beads. The deubiquitination reaction mixtures were proceeded for 1 h at room temperature with rotation for even mixing. At the end, 10 μl 5× SDS sample buffer were added to stop the reaction, and the reaction mixtures were boiled for 10 min before gel electrophoresis and immunoblotting for ubiquitin and MYCN.

### Antibodies

The antibodies used in this study were as follows: anti-USP28 (17707-1-AP, 1:1000 WB, 1:200 IHC, Proteintech); anti-MYCN (51705S, 1:1000 WB, 1:200 IHC, Cell Signaling

Technology); anti-MYCN (sc-53993, 1:200 WB, Santa Cruz Biotechnology); anti-c-MYC (sc-40, 1:200 WB, Santa Cruz Biotechnology); anti-CyclinD1 (2922S, 1:1000 WB, Cell Signaling); anti-PARP (9542P, 1:1000 WB, Cell Signaling); anti-cleaved PARP (9664S, 1:1000 WB, Cell Signaling); anti-Flag (F3165 1:5000 WB, Sigma); anti-Flag (20543-1-AP, 1:2000 WB, Proteintech); anti-HA (901,503, 1:1000 WB, Bio-Legend); anti-Ub (SC-8017, 1:200 WB, Santa Cruz Biotechnology); anti-LSD1 (20813-1-AP, 1:1000 WB, Proteintech); anti-Ki67 (27309-1-AP, 1:1000 WB, Proteintech); anti-Actin (66009-1-Ig, 1:5000 WB, Proteintech); and anti-GAPDH (60004-1-Ig, 1:5000 WB, Proteintech); the secondary antibodies conjugated to horseradish peroxidase were used for Western blotting. The secondary antibodies of anti-mouse or anti-rabbit containing Alexa Fluor 488 or 594 were used for immunofluorescence staining (Jackson ImmunoResearch Laboratories).

### *Statistical analysis*

The results are presented as the mean ± SD. The data were analyzed using GraphPad Prism 9.0 and ImageJ. Unpaired Student *t* tests were performed for comparisons between two groups. All experiments were repeated at least three times.

## Data availability

All data are contained within this article and available from the corresponding author on reasonable request.

*Acknowledgments*—We thank the core facility in Zhejiang Provincial Key Laboratory of Pancreatic Disease for help with various instruments. The authors are in debt to Mr Shenghui Hong for excellent animal support.

*Author contributions*—J. L. and J. P. methodology; J. L., L. W., X. S., X. Z., Y. Z., H. M., Y. X., Q. X., and J. P. investigation; J. L., Q. Z., and P. Z. data analyses; J. L., Q. Z. and P. Z. writing-original draft; J. L., J. P., Q. Z., P. Z., L. W., X. S., X. Z., Y. Z., H. M., Y. X., and Q. X. writing–review and editing.

*Funding and additional information*—This work was supported by grants from the National Natural Science Foundation of China (81773032, 81874223 and 82073481), and the National Key R&D Program of China (2018YFA0507500).

*Conflict of interest*—The authors declare that they have no conflict of interest with the contents of this article.

*Abbreviations*—The abbreviations used are: *MYCC*, *c-Myc*; NB, neuroblastoma; PDX, patient-derived xenograft; USP28, ubiquitin specific protease 28.

## References

1. Maris, J. M., Hogarty, M. D., Bagatell, R., and Cohn, S. L. (2007) Neuroblastoma. *Lancet* **369**, 2106–2120
2. Huang, M., and Weiss, W. A. (2013) Neuroblastoma and MYCN. *Cold Spring Harb. Perspect. Med.* **3**, a014415
3. Matthay, K. K., Maris, J. M., Schleiermacher, G., Nakagawara, A., Mackall, C. L., Diller, L., *et al.* (2016) Neuroblastoma. *Nat. Rev. Dis. Primers* **2**, 16078
4. Castleberry, R. P. (1997) Neuroblastoma. *Eur. J. Cancer* **33**, 1430–1437. Discussion 1437-1438
5. Molenaar, J. J., Koster, J., Zwijnenburg, D. A., van Sluis, P., Valentijn, L. J., van der Ploeg, I., *et al.* (2012) Sequencing of neuroblastoma identifies chromothripsis and defects in neuritogenesis genes. *Nature* **483**, 589–593
6. Mossé, Y. P., Laudenslager, M., Longo, L., Cole, K. A., Wood, A., Attiyeh, E. F., *et al.* (2008) Identification of ALK as a major familial neuroblastoma predisposition gene. *Nature* **455**, 930–935
7. Honda, R., Tanaka, H., and Yasuda, H. (1997) Oncoprotein MDM2 is a ubiquitin ligase E3 for tumor suppressor p53. *FEBS Lett.* **420**, 25–27
8. George, R. E., Sanda, T., Hanna, M., Fröhling, S., Luther, W., 2nd, Zhang, J., *et al.* (2008) Activating mutations in ALK provide a therapeutic target in neuroblastoma. *Nature* **455**, 975–978
9. Fredlund, E., Ringnér, M., Maris, J. M., and Påhlman, S. (2008) High Myc pathway activity and low stage of neuronal differentiation associate with poor outcome in neuroblastoma. *Proc. Natl. Acad. Sci. U. S. A.* **105**, 14094–14099
10. Brodeur, G. M., Seeger, R. C., Schwab, M., Varmus, H. E., and Bishop, J. M. (1984) Amplification of N-myc in untreated human neuroblastomas correlates with advanced disease stage. *Science* **224**, 1121–1124
11. Schwab, M., Varmus, H. E., Bishop, J. M., Grzeschik, K. H., Naylor, S. L., Sakaguchi, A. Y., *et al.* (1984) Chromosome localization in normal human cells and neuroblastomas of a gene related to c-myc. *Nature* **308**, 288–291
12. Zajac-Kaye, M. (2001) Myc oncogene: a key component in cell cycle regulation and its implication for lung cancer. *Lung Cancer* **34 Suppl 2**, S43–S46
13. Bretones, G., Delgado, M. D., and León, J. (2015) Myc and cell cycle control. *Biochim. Biophys. Acta* **1849**, 506–516
14. Lemaitre, J. M., Buckle, R. S., and Méchali, M. (1996) c-Myc in the control of cell proliferation and embryonic development. *Adv. Cancer Res.* **70**, 95–144
15. Vita, M., and Henriksson, M. (2006) The Myc oncoprotein as a therapeutic target for human cancer. *Semin. Cancer Biol.* **16**, 318–330
16. Felgenhauer, J., Tomino, L., Selich-Anderson, J., Bopp, E., and Shah, N. (2018) Dual BRD4 and AURKA inhibition is synergistic against MYCN-amplified and nonamplified neuroblastoma. *Neoplasia* **20**, 965–974
17. Maser, T., Zagorski, J., Kelly, S., Ostrander, A., Goodyke, A., Nagulapally, A., *et al.* (2020) The MDM2 inhibitor CGM097 combined with the BET inhibitor OTX015 induces cell death and inhibits tumor growth in models of neuroblastoma. *Cancer Med.* **9**, 8144–8158
18. Allen-Petersen, B. L., and Sears, R. C. (2019) Mission possible: advances in MYC therapeutic targeting in cancer. *BioDrugs* **33**, 539–553
19. Prieto-Garcia, C., Tomašković, I., Shah, V. J., Dikic, I., and Diefenbacher, M. (2021) USP28: oncogene or tumor suppressor? a unifying paradigm for squamous cell carcinoma. *Cells* **10**, 2652
20. Wu, Y., Wang, Y., Yang, X. H., Kang, T., Zhao, Y., Wang, C., *et al.* (2013) The deubiquitinase USP28 stabilizes LSD1 and confers stem-cell-like traits to breast cancer cells. *Cell Rep.* **5**, 224–236
21. Popov, N., Wanzel, M., Madiredjo, M., Zhang, D., Beijersbergen, R., Bernards, R., *et al.* (2007) The ubiquitin-specific protease USP28 is required for MYC stability. *Nat. Cell Biol.* **9**, 765–774
22. Diefenbacher, M. E., Popov, N., Blake, S. M., Schülein-Völk, C., Nye, E., Spencer-Dene, B., *et al.* (2014) The deubiquitinase USP28 controls intestinal homeostasis and promotes colorectal cancer. *J. Clin. Invest.* **124**, 3407–3418
23. Flügel, D., Görlach, A., and Kietzmann, T. (2012) GSK-3β regulates cell growth, migration, and angiogenesis via Fbw7 and USP28-dependent degradation of HIF-1α. *Blood* **119**, 1292–1301
24. Sun, X., Cai, M., Wu, L., Zhen, X., Chen, Y., Peng, J., *et al.* (2022) Ubiquitin-specific protease 28 deubiquitinates TCF7L2 to govern the action of the Wnt signaling pathway in hepatic carcinoma. *Cancer Sci.* **113**, 3463–3475
25. Cremona, C. A., Sancho, R., Diefenbacher, M. E., and Behrens, A. (2016) Fbw7 and its counteracting forces in stem cells and cancer: oncoproteins in the balance. *Semin. Cancer Biol.* **36**, 52–61
26. Diefenbacher, M. E., Chakraborty, A., Blake, S. M., Mitter, R., Popov, N., Eilers, M., *et al.* (2015) Usp28 counteracts Fbw7 in intestinal homeostasis and cancer. *Cancer Res.* **75**, 1181–1186

27. Peng, J., Jiang, K., Sun, X., Wu, L., Wang, J., Xi, X., *et al.* (2022) Identification of a class of potent USP25/28 inhibitors with broad spectrum of anti-tumor activity. *Signal Transduct. Target. Ther.* **7**, 393
28. Popov, N., Herold, S., Llamazares, M., Schülein, C., and Eilers, M. (2007) Fbw7 and Usp28 regulate myc protein stability in response to DNA damage. *Cell Cycle* **6**, 2327–2331
29. Schweigerer, L., and Fotsis, T. (1991) [Increased expression of the MYCN oncogene in human neuroblastoma cells and possible, new therapeutic approaches]. *Klin. Padiatr.* **203**, 319–322
30. Chan, H. S., Gallie, B. L., DeBoer, G., Haddad, G., Ikegaki, N., Dimitroulakos, J., *et al.* (1997) MYCN protein expression as a predictor of neuroblastoma prognosis. *Clin. Cancer Res.* **3**, 1699–1706
31. Wang, L., Chen, C., Song, Z., Wang, H., Ye, M., Wang, D., *et al.* (2022) EZH2 depletion potentiates MYC degradation inhibiting neuroblastoma and small cell carcinoma tumor formation. *Nat. Commun.* **13**, 12
32. Schmelz, K., Toedling, J., Huska, M., Cwikla, M. C., Kruetzfeldt, L. M., Proba, J., *et al.* (2021) Spatial and temporal intratumour heterogeneity has potential consequences for single biopsy-based neuroblastoma treatment decisions. *Nat. Commun.* **12**, 6804
33. Tucker, E. R., Danielson, L. S., Innocenti, P., and Chesler, L. (2015) Tackling Crizotinib resistance: the pathway from drug discovery to the pediatric clinic. *Cancer Res.* **75**, 2770–2774
34. Boeva, V., Louis-Brennetot, C., Peltier, A., Durand, S., Pierre-Eugène, C., Raynal, V., *et al.* (2017) Heterogeneity of neuroblastoma cell identity defined by transcriptional circuitries. *Nat. Genet.* **49**, 1408–1413
35. Tavana, O., Li, D., Dai, C., Lopez, G., Banerjee, D., Kon, N., *et al.* (2016) HAUSP deubiquitinates and stabilizes N-Myc in neuroblastoma. *Nat. Med.* **22**, 1180–1186
36. Schulte, J. H., Lim, S., Schramm, A., Friedrichs, N., Koster, J., Versteeg, R., *et al.* (2009) Lysine-specific demethylase 1 is strongly expressed in poorly differentiated neuroblastoma: implications for therapy. *Cancer Res.* **69**, 2065–2071
37. Luo, J., Solimini, N. L., and Elledge, S. J. (2009) Principles of cancer therapy: oncogene and non-oncogene addiction. *Cell* **136**, 823–837
38. Prieto-Garcia, C., Hartmann, O., Reissland, M., Braun, F., Fischer, T., Walz, S., *et al.* (2020) Maintaining protein stability of ΔNp63 via USP28 is required by squamous cancer cells. *EMBO Mol. Med.* **12**, e11101
39. Wang, J., Dong, Y., Ma, H., Wu, L., Zhen, X., Tang, L., *et al.* (2022) The deubiquitinase USP28 stabilizes the expression of RecQ family helicases and maintains the viability of triple negative breast cancer cells. *J. Biol. Chem.* **298**, 101443
40. Shen, J., Xie, M., Xu, Y., Qian, Q., Qiu, T., Shi, W., *et al.* (2022) Identification of the deubiquitinase USP28 as a novel molecular therapeutic target of ovarian cancer. *Biochem. Biophys. Res. Commun.* **638**, 184–191
41. Peng, J., Tang, L., Cai, M., Chen, H., Wong, J., and Zhang, P. (2019) RECQL5 plays an essential role in maintaining genome stability and viability of triple-negative breast cancer cells. *Cancer Med.* **8**, 4743–4752